J. Fluid Mech. (1985), *vol.* 158, *pp.* 365–380
Printed in Great Britain

Analytical prediction of the transition from Mach to regular reflection over cylindrical concave wedges

By G. BEN-DOR
Department of Mechanical Engineering, Ben-Gurion University of the Negev, Beer Sheva, Israel
AND K. TAKAYAMA
Institute of High Speed Mechanics, Tohoku University, Sendai, Japan

(Received 30 June 1984)

Two formulas, based on analytical considerations, which are capable of predicting the wedge angle of transition from Mach to regular reflection over cylindrical concave wedges, are developed. They are derived using Hornung, Oertel & Sandeman's (1979) conclusion that a Mach reflection can exist only if the corner-generated signals can catch up with the incident shock wave. The good agreement between the present models and the experimental results confirm Hornung *et al.*'s (1979) concept. The predictions of these models are in better agreement with experimental results than the predictions of Itoh, Okazaki & Itaya's (1981) model. The present models are very simple to use and apply but, like Itoh *et al.*'s (1981) model, they also lack the ability to account for the dependence of the transition angle on the radius of curvature of the cylindrical wedge.

1. Introduction

The reflection of oblique shock waves is a nonlinear problem which has been investigated analytically and experimentally by many researchers. Results of investigations in the past decade indicate that the phenomenon can be divided into three categories, depending on whether the flow is steady, pseudo-steady or truly unsteady (Ben-Dor 1980; Ben-Dor & Glass 1979 and Ben-Dor, Takayama & Kawauchi 1980, respectively). The reflection phenomenon in truly unsteady flows has caught the attention of many investigators in recent years because of (1) the desire to understand more about the reflection of spherical shock waves which belong to the truly unsteady flow category, and (2) the fact that actual transition can occur only in flows which are truly unsteady.

Figure 1 illustrates three different types of truly unsteady reflections. In figure 1 (*a*) the reflection of a spherical shock wave is shown. When the blast wave first collides with the ground surface it experiences a head-on collision ($\theta_w = 90°$) immediately followed by a regular reflection. As the blast wave propagates outwards it attenuates and the reflecting wedge angle θ_w at the reflection point decreases until the regular reflection goes through a transition to a Mach reflection (for very strong blast waves the sequence of events will be regular reflection → double-Mach reflection → complex-Mach reflection and, finally, single-Mach reflection).

A similar situation is shown in figure 1 (*b*). Here a planar normally incident shock

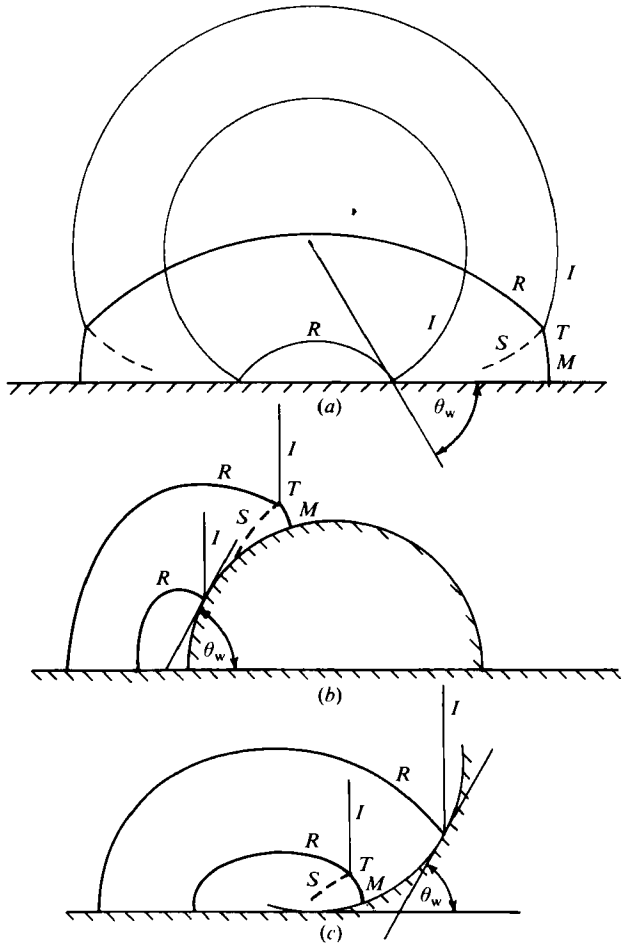

FIGURE 1. Three different types of truly unsteady shock-wave reflection: (*a*) spherical-blast-wave reflection over a plane surface; (*b*) planar-shock-wave reflection over a cylindrical convex wedge; and (*c*) planar-shock-wave reflection over a cylindrical concave wedge. For each case the wave configurations of both the regular reflection (RR) and the Mach reflection (MR) are illustrated. *I*, incident shock wave; *R*, reflected shock wave; *M*, Mach stem; *T*, triple point and θ_w, reflecting wedge angle.

wave, propagating from left to right, collides with a convex half-cylinder. Again, initially the shock wave experiences a head-on collision. As the shock wave propagates up the wedge, the reflecting wedge angle θ_w at the reflection point decreases until the regular reflection goes through a transition to a Mach reflection. Unlike the previous case of a blast wave (figure 1*a*), where both the incident-shock-wave Mach number and the reflecting wedge angle decrease as the blast wave propagates, here only the reflecting wedge angle decreases while the incident-shock-wave Mach number remains constant.

An opposite transition process is shown in figure 1(*c*). Here the planar normally incident shock wave, propagating from left to right, collides with a concave half-cylinder. Initially, the shock wave is reflected as a Mach reflection. However, as the shock wave propagates up the wedge the reflecting wedge angle θ_w increases, to result in transition to regular reflection. As in figure 1(*b*) the incident-shock-wave Mach number remains constant while the reflecting wedge angle changes.

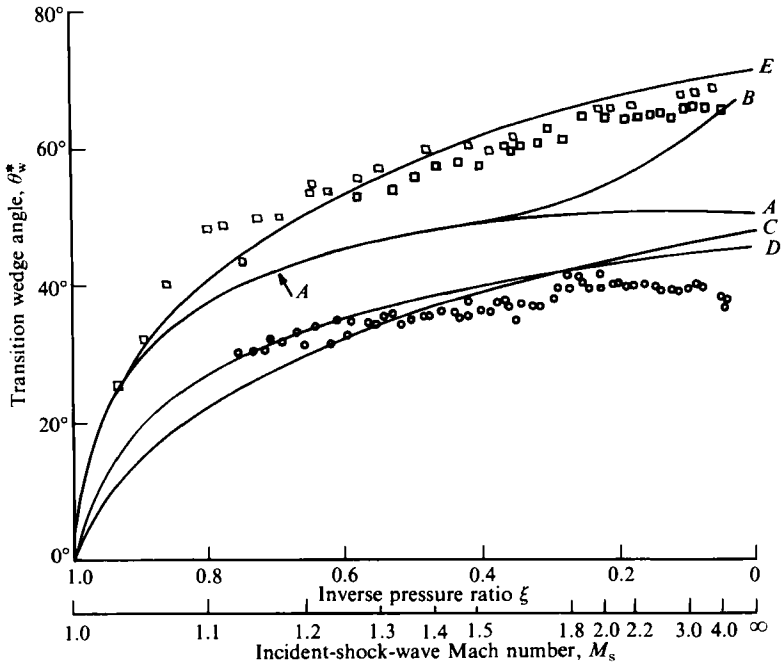

FIGURE 2. Transition from MR to RR and from RR to MR in the (ξ, θ_w)-plane, experimental results and some theoretical transition lines. ξ is the inverse pressure ratio across the incident shock wave; θ_w is the wedge angle; ○, RR→MR transition over convex cylinders (figure 1*b*); □, MR→RR transition over concave cylinders (figure 1*c*). Line *A*, the 'detachment' criterion of von Neumann (1963); *B*, the 'mechanical-equilibrium' criterion of Henderson & Lozzi (1975); *C*, Heilig's (1969) RR→MR transition over convex cylinders; *D*, Itoh, Okazaki & Itaya's (1981) RR→MR transition over convex wedges; *E*, Itoh, Okazaki & Itaya's (1981) MR→RR transition over concave wedges.

Heilig (1969) was probably the first to study the reflection of a planar shock wave over cylindrical (figure 1*b*) and elliptical convex wedges. The measured transition wedge angles obtained in his study are shown in figure 2 (circles). Ben-Dor *et al.* (1980) confirmed Heilig's experimental results using a more accurate measuring technique, namely streak photography with curved slits (for details see Ben-Dor & Takayama 1981). Their experimental study was extended to include the reflection of a planar shock wave over a cylindrical concave wedge (figure 1*c*). The measured transition wedge angles for this case are shown by squares in figure 2. It is clearly seen that the RR→MR transition over a convex cylinder occurs at wedge angles which are significantly smaller than those appropriate to the MR→RR transition over a concave cylinder. Following this study Takayama & Ben-Dor (1984) proposed a possible hysteresis loop for the RR⇌MR transition phenomenon.

Soon after Ben-Dor *et al.*'s (1980) results were published, a new study along the same line of investigation by Itoh *et al.* (1981) was reported. They repeated the experimental study of Ben-Dor *et al.* (1980) and added a numerical analysis. Using Milton's (1975) modification of Whitham's (1957) theory, they numerically calculated the transition wedge angle for the RR→MR transition over a cylindrical convex wedge and for the MR→RR transition over a cylindrical concave wedge. These numerical transition curves are shown in figure 2 as curves *D* and *E*, respectively. Curve *C* in figure 2 was numerically calculated by Heilig (1969), who applied Whitham's (1957) classical theory. A comparison between curves *C* and *D* and the experimental results (open circles) indicates that Milton's (1975) modification of

Whitham's theory does improve the agreement between the numerical predictions and the experimental results.

The other two curves in figure 2, A and B, respectively represent the 'detachment' criterion of von Neumann (1963), which is the RR$\rightleftharpoons$MR transition criterion in pseudo-steady flows, and the 'mechanical equilibrium' criterion of Henderson & Lozzi (1975), which is the RR$\rightleftharpoons$MR transition criterion in steady flows. The difference in the transition criterion between steady and pseudo-steady flows was explained physically by Hornung *et al.* (1979).

Aside from the fact that the numerical transition curves (C, D and E in figure 2) fail to predict accurately the actual transition wedge angles, they pose some additional difficulties: (1) the numerical procedure involved in calculating each curve is quite complex; (2) the numerical transition curves fail to account for the radius of curvature of the cylindrical wedges; and (3) the numerical transition curves fail to account for the angle of incidence of the cylindrical wedges.

The dependence of the transition wedge angle on the radius of curvature of the wedge was studied by Takayama & Sasaki (1983) and Dewey *et al.* (1983) for both convex and concave cylindrical wedges. Itoh & Itaya (1981) investigated the effect of the angle of incidence of a cylindrical concave wedge on the transition wedge angle.

These studies indicated that, as the angle of incidence and/or the radius of curvature of a cylindrical concave wedge are increased, the actual transition wedge angles decrease and approach the values predicted by the 'mechanical-equilibrium' transition line (the squares in figure 2 approach curve B). On the other hand, in the case of a cylindrical convex wedge, an increase in the radius of curvature causes an increase in the actual transition wedge angle, which approaches the 'detachment' transition line (the circles in figure 2 approach curve A). Note that when $R \rightarrow \infty$ both the concave and convex cylindrical wedges approach (from a geometrical point of view) the case of a straight wedge.

In the following, two expressions, based on analytical concepts, for predicting the MR$\rightarrow$RR transition wedge angles over cylindrical concave wedges are developed. Furthermore, it will be shown that the criteria developed here fit well with the so-called 'general criterion' for the RR$\rightleftharpoons$MR transition in steady, pseudo-steady and truly unsteady flows, which was first suggested by Hornung *et al.* (1979).

2. Present analysis

The aim of the present analysis is to obtain the MR$\rightarrow$RR transition line of a planar shock wave over a cylindrical concave wedge by applying Hornung *et al.*'s (1979) 'corner-signal' concept. This suggested that, for a Mach reflection to exist, the corner signals generated at the tip of the reflecting wedge must catch up with the incident shock wave. This concept implies that, if the corner-generated signals cannot catch up with the incident shock wave, then a Mach reflection cannot exist. Instead the reflection will be regular. This is due to the fact that a regular reflection is a type of reflection which can be isolated from the tip of the wedge in the sense that it does not need to know about the existence of the tip of the wedge where the reflection actually started. Hornung *et al.* (1979) proved this concept to be valid for both steady and pseudo-steady shock-wave reflections. In the case of a pseudo-steady reflection they clearly showed that transition from regular to Mach reflection can occur only after the corner-generated signals catch up with the incident shock wave (at the reflection point). If, however, the corner-generated signals cannot catch up with the reflection point a Mach reflection is unobtainable.

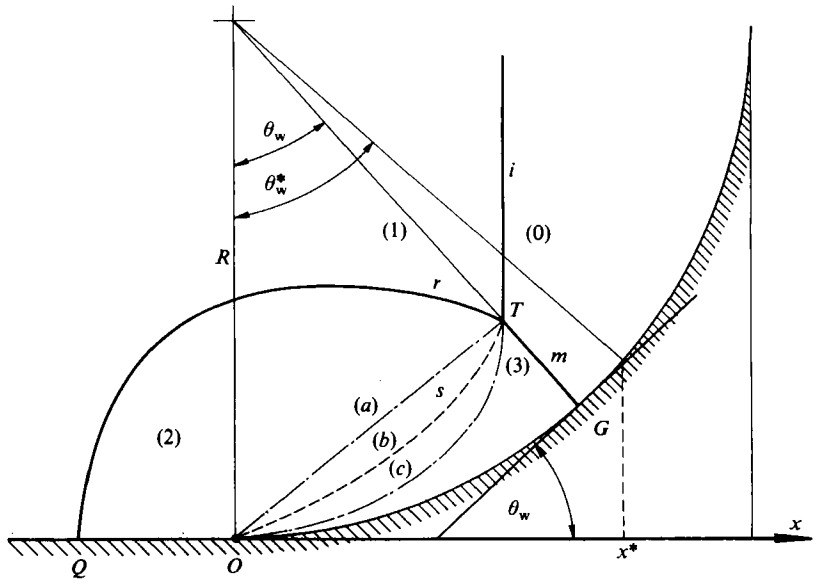

FIGURE 3. Schematic illustration of a Mach reflection over a cylindrical concave wedge.

When a planar-incident shock wave encounters a cylindrical concave wedge it initially reflects as a Mach reflection. A schematic drawing of such a Mach reflection is shown in figure 3. The information about the disturbance caused by the wedge is limited to the area bounded by the Mach stem m and the reflected shock wave r, i.e. regions (2) and (3). Following Hornung *et al.* (1979) one must conclude that, since the initial reflection is a Mach reflection, the corner signals, which were generated at the instant when the incident shock wave collided with the tip of the wedge, were able to catch up with the incident shock wave i (at the triple point T).

The path along which the corner-generated signals propagate on their way to catch up with the triple point is unknown. It is only known that the corner-generated signals are moving with speed $u+a$, where u is the flow velocity and a the local speed of sound, and that when they catch up with the incident shock wave they are swallowed by it, i.e. they stop moving with speed $u+a$ and start moving with the shock speed. The actual path along which the corner-generated signals propagate can be along any line connecting the tip of the wedge, point 0, and the triple point T, provided the line passes through subsonic-flow regions.

As the incident shock wave propagates over the cylindrical concave wedge, the Mach reflection terminates to form a regular reflection. Following Hornung *et al.* (1979) it can be assumed that the termination of the Mach reflection occurs at the point where it becomes impossible for the corner-generated signals to catch up with the incident shock wave.

Figure 4 illustrates a regular reflection exactly at the point where the MR→RR transition occurred. At earlier times (or positions) a Mach reflection (similar to the one shown schematically in figure 3 and actually in figure 5*a*) existed. The corner-generated signals were able to catch up with the incident shock wave of this Mach reflection, be swallowed by it and continue to propagate with it. However, since the concave wedge is becoming more and more steep as the incident shock wave continues to propagate, the corner-generated signals are losing in their race to catch up with the incident shock wave, and eventually they fall back behind it.

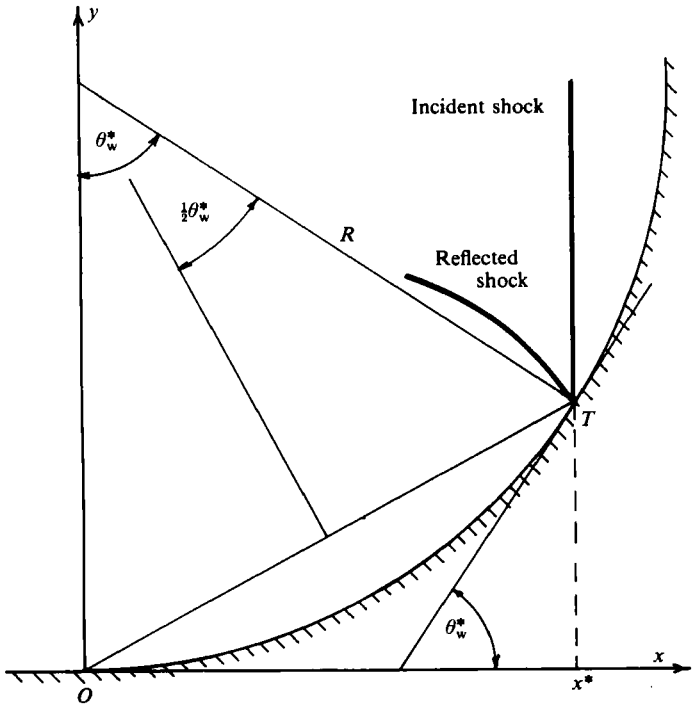

FIGURE 4. A Mach reflection over a concave cylinder exactly at transition: O, tip of the wedge; T, triple point; R, radius of curvature of the wedge; θ_w^*, transition wedge angle; x^*, distance travelled by the incident shock wave from the tip of the wedge to the point where transition occurred.

At times (or positions) beyond the situation shown in figure 4 (which corresponds to the position where the MR→RR transition occurs), the corner-generated signals are no longer able to catch up with the incident shock wave, and hence a Mach reflection becomes impossible. The actual reflection which is obtained after the termination of the Mach reflection (shown in figure 5*a*) is shown in figure 5*b*. The incident shock wave is clearly seen to reflect regularly from the wedge. The reflected shock wave extends backwards and forms a new triple point. A short shock wave which emanates from this triple point terminates perpendicularly on the wedge surface. The flow bounded by the reflected shock wave, the wedge surface and the short normal shock wave is supersonic. Consequently, the short normal shock wave actually indicates the exact position to which the corner-generated signals have propagated. The corner-generated signals cannot precede this normal shock wave; they are swallowed by it and continue to propagate with its velocity. Thus, the reflection point of the regular reflection (as well as the incident shock wave) is isolated from the corner-generated signals by a supersonic flow region. The corner signals generated at the tip of the wedge (point O) are moving with a velocity $u+a$. In general, the value of $u+a$ changes inside the flow field. If Δt is the time for the incident shock wave to travel from $x = 0$ to x^*, where x^* is the point where the corner-generated signals had caught up with the triple point T, then the corner signals have propagated during this time a distance of

$$S = \int_0^{\Delta t} (u+a)\,\mathrm{d}t. \tag{1}$$

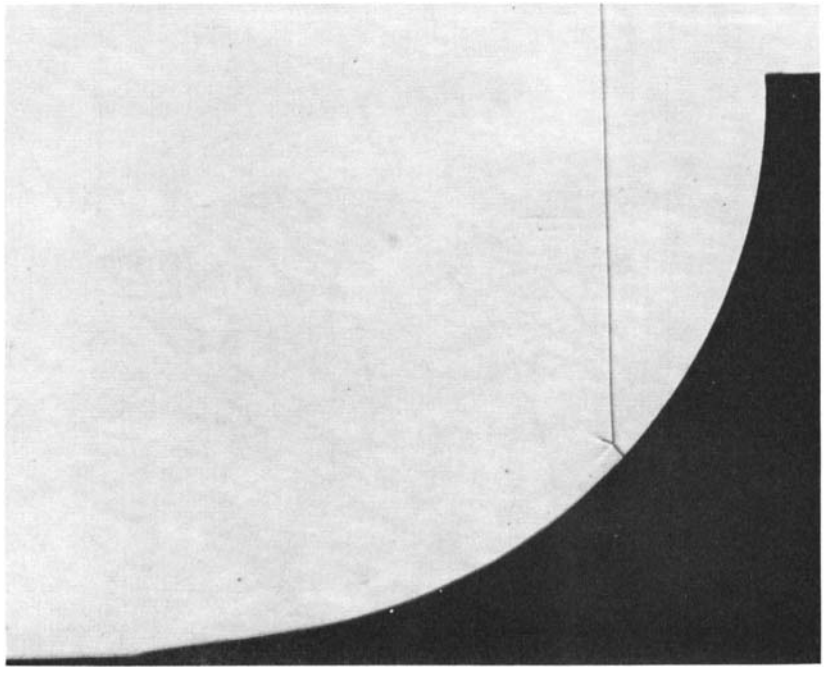

(*a*)

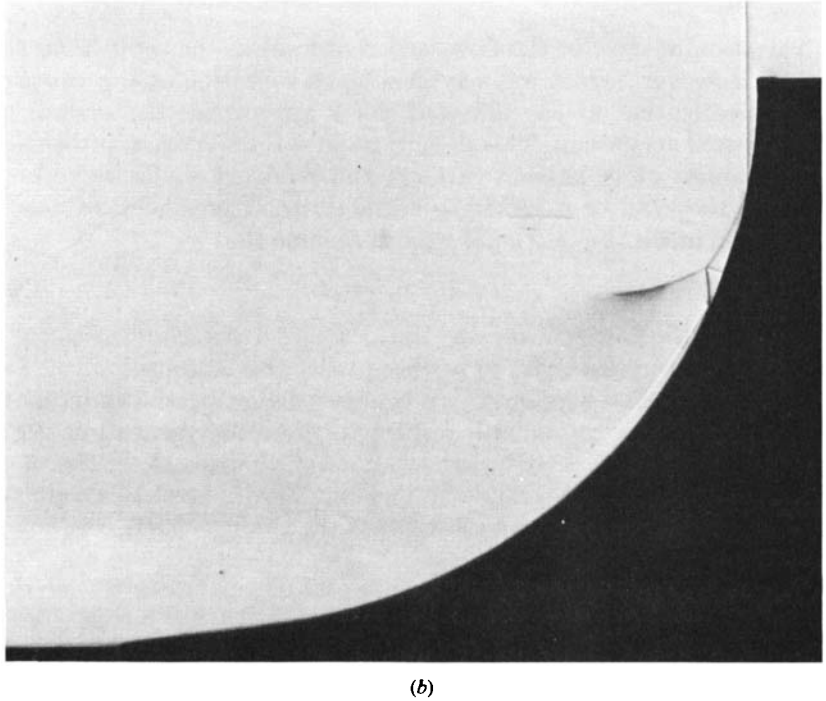

(*b*)

FIGURE 5. Direct shadowgraphs of reflection over cylindrical concave wedges: (*a*) Mach reflection; (*b*) regular reflection. Incident-shock-wave Mach number $M_s = 1.48$; initial pressure $P_0 = 1.667 \times 10^4$ Pascal; initial temperature $T_0 = 292$ K; radius of curvature $R = 50$ mm. The test gas is dry air.

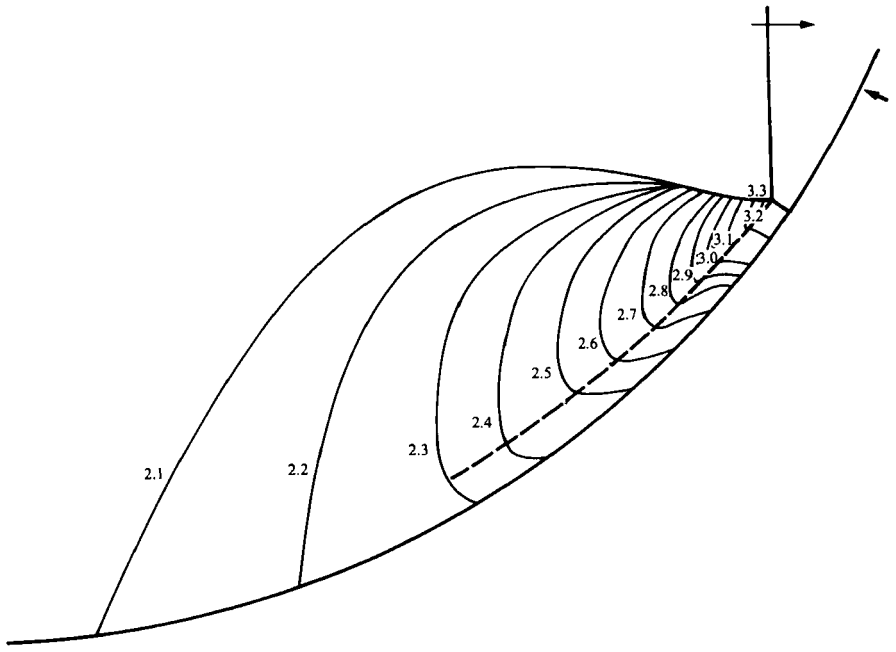

FIGURE 6. Isopycnics of a Mach reflection in dry air over a concave cylinder: $M_s = 1.57$; $P_0 = 1.667 \times 10^4$ Pascal; $T_0 = 295$ K; $R = 50$ mm. The numbers indicate density ratios with respect to the density ahead of the incident shock wave.

Since the variation of $u+a$ in the flow field is unknown, the right-hand side of (1) is unsolvable. However, inspecting a typical Mach reflection over a concave wedge (figure 5*a*) indicates that as the reflected shock approaches the surface (point Q, figure 3) it becomes very weak. This in turn implies that the flow properties do not change significantly while passing through the reflected shock wave at point Q (figure 3). Thus they can be assumed to maintain their pre-shock values (i.e. their values behind the incident shock) and we can assume that

$$u+a = u_1+a_1, \tag{2}$$

where u_1 and a_1 are the flow velocity and the local speed of sound behind the incident shock wave, respectively. In order to further justify this assumption, the isopycnics corresponding to a Mach reflection over a concave wedge are shown in figure 6. The numbers indicate density ratios with respect to the density ahead of the incident shock wave. It can be seen clearly that the density changes along the wedge from about 2.1 (which is the value behind the incident shock wave) to a value of about 3.0 behind the Mach stem, thus suggesting that the changes inside the flow field are not too large.

Once the assumption of (2) is used, the integration of (1) can be carried out, to result in

$$S = (u_1+a_1)\,\Delta t. \tag{3}$$

Unfortunately, the exact path of propagation of the corner-generated signals is also unknown. Consequently the value of S in (3) is itself unknown.

In the following, two possible propagation paths will be examined. The first is along the straight line connecting the tip of the wedge O and the triple point T, i.e. line $\overline{OT}$. The second path is along the slipstream s on either side of it. Both of these lines

are shown in figure 3, as (*a*) and (*b*), respectively. It should be noted again that the actual line need not be any of these lines. It can be any line connecting points O and T, e.g. line (*c*) in figure 3.

3. Propagation path along either side of the slipstream – (model *A*)

Let us assume that the corner signals propagate from the tip of the wedge (point O) to the triple point T along the slipstream on either side of it (dashed line in figure 3). As a first approximation we assume that the length of this propagation path is very close to the length of the circular arc $\widehat{OG}$. Inspecting a photograph of a Mach reflection over a concave wedge such as the one shown in figure 5(*a*) indicates that the Mach stem is quite short compared with the radius of curvature of the wedge, and hence the above approximation is quite good. Furthermore the Mach stem, which is perpendicular to the cylindrical wedge surface, coincides with the radius of curvature, and therefore one can write

$$S = R\theta_{\mathrm{w}}, \tag{4}$$

where R is the wedge radius of curvature.

Inserting (4) into (3) results in

$$R\theta_{\mathrm{w}} = (u_1 + a_1)\,\Delta t. \tag{5}$$

If, however, the instant of transition is considered, i.e. if $\Delta t = x^*/u_{\mathrm{s}}$, where x^* is the x-coordinate where transition occurs (i.e. the point beyond which the corner-generated signals cannot catch up with the incident shock wave i) then (5) should be replaced by

$$R\theta_{\mathrm{w}}^* = (u_1 + a_1)\frac{x^*}{u_{\mathrm{s}}}, \tag{6}$$

where θ_{w}^* is the wedge angle at the point where transition occurs.

From figure 3

$$x^* = R\sin\theta_{\mathrm{w}}^*. \tag{7}$$

Combining (4), (6) and (7) results in

$$\frac{\sin\theta_{\mathrm{w}}^*}{\theta_{\mathrm{w}}^*} = \frac{u_{\mathrm{s}}}{u_1 + a_1}. \tag{8}$$

Dividing both the numerator and the denominator on the right-hand side by the local speed of sound a_0 of the flow ahead of the incident shock wave finally results in

$$\frac{\sin\theta_{\mathrm{w}}^*}{\theta_{\mathrm{w}}^*} = \frac{M_{\mathrm{s}}}{U_{10} + A_{10}}, \tag{9}$$

where M_{s} is the incident-shock-wave Mach number, $U_{10} = u_1/a_0$ and $A_{10} = a_1/a_0$. Note that, for moderate shock-wave Mach numbers, U_{10} and A_{10} are functions of the incident-shock-wave Mach number only through the following relations:

$$U_{10} = \frac{2(M_{\mathrm{s}}^2 - 1)}{(\gamma + 1)\,M_{\mathrm{s}}} \tag{10}$$

and

$$A_{10} = \frac{\gamma - 1}{\gamma + 1}\frac{1}{M_{\mathrm{s}}}\left[\frac{2\gamma}{\gamma - 1}(M_{\mathrm{s}}^2 - 1)\left(M_{\mathrm{s}}^2 + \frac{2}{\gamma - 1}\right)\right]^{\frac{1}{2}}, \tag{11}$$

where γ is the specific-heat ratio, i.e. $\gamma = \frac{7}{5}$ for a diatomic perfect gas and $\gamma = \frac{5}{3}$ for a monatomic perfect gas.

4. Propagation path along the straight line $\overline{OT}$ – (model *B*)

This time we assume that the corner-generated signals propagate along the shortest path connecting the tip of the wedge (point O) and the triple point T. Again we assume as a first approximation that the length of this propagation path is very close to the length of the line connecting points O and G, i.e. $\overline{OT} \sim \overline{OG}$ (figure 3). This assumption can be again justified by the fact that the length of the Mach stem λ (of a Mach reflection over a cylindrical concave wedge) is very short compared with the radius of curvature R, i.e. $\lambda \ll R$.

The foregoing assumptions, together with the fact that the Mach stem coincides with the radius of curvature, imply

$$\tfrac{1}{2}S = R \sin \tfrac{1}{2}\theta_{\mathrm{w}}. \tag{12}$$

Inserting S from (12) into (3), and then replacing t by x^*/u_{s}, results in

$$\cos \tfrac{1}{2}\theta_{\mathrm{w}}^* = \frac{u_{\mathrm{s}}}{u_1 + a_1}. \tag{13}$$

Again, we non-dimensionalize the right-hand side by the local speed of sound ahead of the incident shock wave to obtain

$$\cos \tfrac{1}{2}\theta_{\mathrm{w}}^* = \frac{M_{\mathrm{s}}}{U_{10} + A_{10}}. \tag{14}$$

In summary, (9) and (14) together with (10) and (11) provide two different expressions of the form $\theta_{\mathrm{w}}^* = \theta_{\mathrm{w}}^*(M_{\mathrm{s}})$ by which the transition wedge angle θ_{w}^* can be calculated for a given incident-shock-wave Mach number M_{s}. While developing these two expressions it was assumed that the speed of propagation of the corner-generated signals remains constant inside the flow field, (2). This assumption enabled us to integrate (1) to obtain (3). In order to carry the present analysis further, the distance S (equation (3)) passed by the corner-generated signals, was expressed using two simple geometrical expressions, which finally enabled us to obtain two simple expressions ((9) and (14)) by which the transition wedge angle θ_{w}^* can be calculated.

Note that (3) requires a value for S. However, there is no need to know the exact path of the corner-generated signals. For example, while replacing S by $R\theta_{\mathrm{w}}$, (4) in the first model, it was not stated that the corner-generated signals propagated along the wedge surface but only that the length of the propagation path could be approximated by $R\theta_{\mathrm{w}}$. For example, it is possible that they propagated along the path labelled (*c*) (in figure 3) which has a length close to $R\theta_{\mathrm{w}}$.

5. Results and discussion

The transition lines predicted by the present two simple models A and B are shown in figure 7 as curves A and B respectively. Recall that curve A was calculated by (9) and curve B by (14). Curve C in figure 7 is the transition line as obtained by Itoh *et al.* (1981) using Milton's (1975) modification of Whitham's (1957) theory. In the following, each of these two models will be discussed separately.

5.1. *Model A*

The agreement between the experimental results and the transition line predicted by this model (9) is quite good in the range $1.1 < M_{\mathrm{s}} < 4.0$. (The upper limit arises from the lack of experimental results with which the model can be compared.) In the range

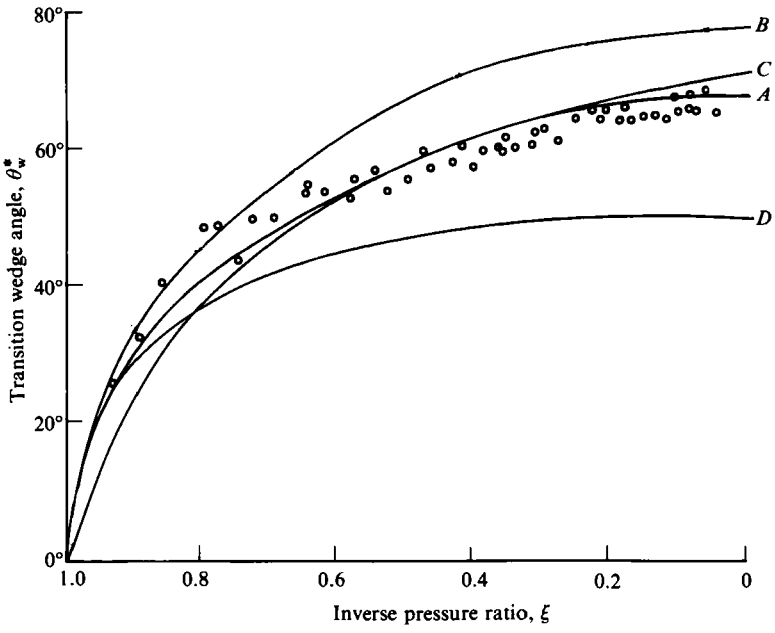

FIGURE 7. Transition from MR→RR over concave cylinders. Circles indicate our experimental measurements for $R = 40$ mm and 50 mm wedges (the initial wedge angle $\theta_w^0 = 0$ for both models). Line A, the transition as predicted by our model A (equation (9)); B, the transition as predicted by our model B (equation (14)); C, the transition as predicted by Itoh *et al.*'s (1981) model which was based on Milton's (1975) modification of Whitham's (1957) theory; D the transition in pseudo-steady flow, i.e. the detachment criterion.

$1.25 < M_s < 2$, curves A and C overlap, i.e. the transition line arising from model A predicts the same transition wedge angles as predicted by Itoh *et al.*'s (1981) numerical study. Both transition lines (A and C) predict higher transition wedge angles than the actual ones. As the incident-shock-wave Mach number increases beyond $M_s = 2$, curve C of Itoh *et al.* (1981) shifts away from the experimental results to predict higher values, while the prediction of the transition line of model A (9) continues to follow the data points with the same accuracy as for the lower Mach numbers. Thus one can conclude that the analytical transition line predicted by model A is in general better than Itoh *et al.*'s (1981) numerical transition line in the range $M_s > 1.1$. In the region $M_s < 1.1$ the predictions of the transition line arising from model A are very poor.

5.2. *Model B*

The agreement between the experimental results and the transition line predicted by this model (14) is good only in the range $1 < M_s < 1.1$. For $M_s > 1.1$, model B predicts transition angles which are greater than the actual transition wedge angles by 10°–15°. It is possible that the reason that the predictions of model B are better at low Mach numbers and those of model A at higher Mach numbers lies in the nature of region (2) (see figure 3). It is known (Ben-Dor 1979) that, as the Mach number of the incident shock wave increases, the Mach number of the flow in region (2) increases until it becomes supersonic. Thus it is possible that the corner-generated signals propagate at low incident-shock-wave Mach numbers from O to T along a path in region (2) which is subsonic. As the Mach number of the incident shock wave increases, the Mach number in region (2) becomes higher and it is possible that the

corner-generated signals prefer now a propagation path in region (3) which is always subsonic.

It is our belief that the lack of very good agreement between the predicted and the actual transition wedge angles is due to the fact that our models are over-simplified compared with the real phenomenon. Nonetheless, the agreement is surprisingly good. In order to get a better agreement one must know the exact distribution of $u+a$ in the entire flow field and the exact path along which the corner-generated signals propagate from point O to the triple point T (figure 3). This would probably require a solution of the conservation equations governing the flow field at hand which is two-dimensional and truly unsteady. Such a solution is extremely difficult. Fortunately, our simplifying assumptions (2) have proven themselves successful. In reality $u+a$ in the flow field at hand is somewhat greater than u_1+a_1. Thus, the corner-generated signals propagate faster and catch up with the reflection point earlier, resulting in smaller transition wedge angles than those predicted by our models A and B. The experimental transition angles which are lower than the predicted ones (figure 7) indicate that this indeed should be the case.

6. The influence of the initial angle of incidence – θ_w^0

Figure 8 illustrates a cylindrical concave wedge which, unlike the one analysed previously, has an initial angle θ_w^0 (note in the previous case $\theta_w^0 = 0$). The procedure involved in developing (9) can be repeated to lead to

$$\frac{\sin\theta_w^* - \sin\theta_w^0}{\theta_w^* - \theta_w^0} = \frac{M_s}{U_{10}+A_{10}}. \tag{15}$$

Three transition lines corresponding to $\theta_w^0 = 0$, 10° and 20° are drawn in figure 9, together with the experimental results of Itoh & Itaya (1979). The experimental results indicate that, the greater the initial wedge angle θ_w^0, the smaller is the value of the transition wedge angle θ_w^*. Increasing θ_w^0 from 0 to 20° causes a general decrease of about 8° in θ_w^*.

The transition lines as predicted by model A exhibit the same trend. However, the agreement between the transition line for a given value of θ_w^0 becomes poorer and poorer as θ_w^0 increases. While the experimental results corresponding to $\theta_w^0 = 0$ are about 2°–3° away from the appropriate transition line, those corresponding to $\theta_w^0 = 10°$ lie about 5°–6° above their transition line and those corresponding to $\theta_w^0 = 20°$ are in general more than 8° away from their transition line. The reason for the fact that, the higher θ_w^0 is, the worse is the agreement between theory and experiments, is probably due to the assumption that $u+a$ is constant and equal to u_1+a_1. When $\theta_w^0 > 0$, the reflected shock wave cannot be assumed anymore to be weak at point Q (figure 3). Thus, $u+a > u_1+a_1$. It should be noted that one might still assume for this case that $u+a =$ constant, but not that $u+a = u_1+a_1$ as assumed in (2). Finally, it is of interest to note that the expression arising from model B, (14), can also be modified to account for θ_w^0. Repeating the procedure with model B and $\theta_w^0 \neq 0$ results in

$$\frac{\sin\theta_w^* - \sin\theta_w^0}{\sin\frac{1}{2}(\theta_w^* - \theta_w^0)} = 2\frac{M_s}{U_{10}+A_{10}}. \tag{16}$$

Owing to the poor agreement between the transition line as predicted by model B at $M_s > 1.1$ and the fact that there are no experimental results for $\theta_w^0 \neq 0$ at $M_s < 1.1$, the transition lines arising from (16) for $\theta_w^0 \neq 0$ are not drawn. However, calculations for $\theta_w^0 = 10°$ and 20° indicate that for this case too θ_w^* decreases as θ_w^0 increases.

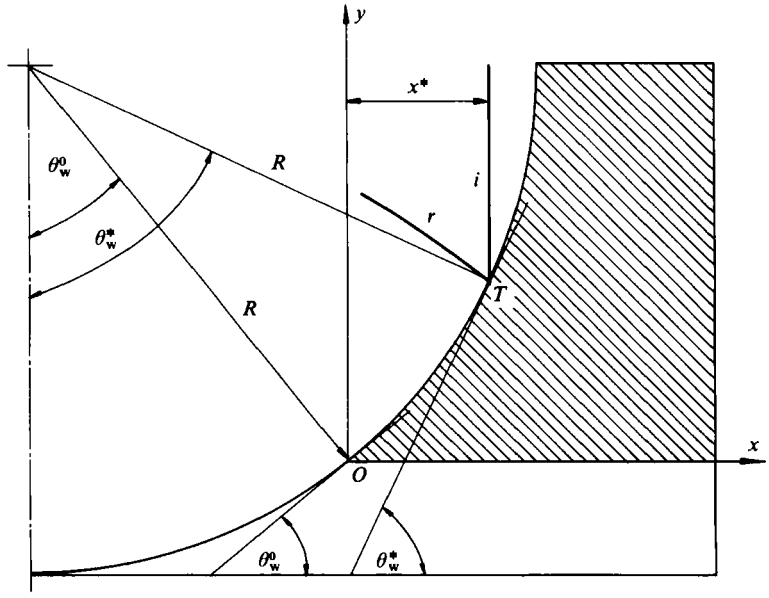

FIGURE 8. Schematic illustration of a Mach reflection over a cylindrical concave wedge exactly at transition: O, tip of the wedge; T, triple point; R, radius of curvature of the wedge; θ_w^*, transition wedge angle; θ_w^0, initial wedge angle; x^*, distance travelled by the incident shock wave from the tip of the wedge to the point where transition occurred.

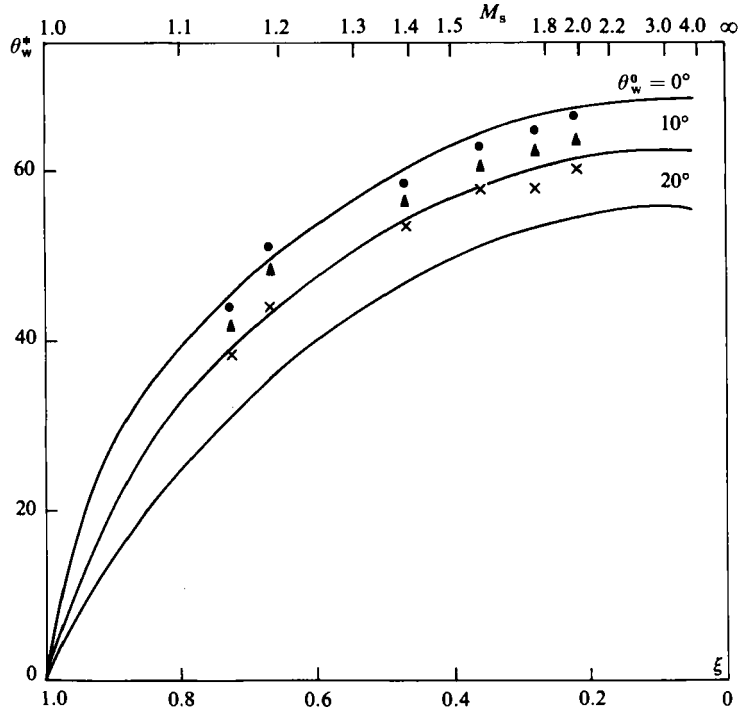

FIGURE 9. Comparison of the transition lines as predicted by model A for $\theta_w^0 = 0$, 10° and 20° with the experimental results of Itoh & Itaya (1979).

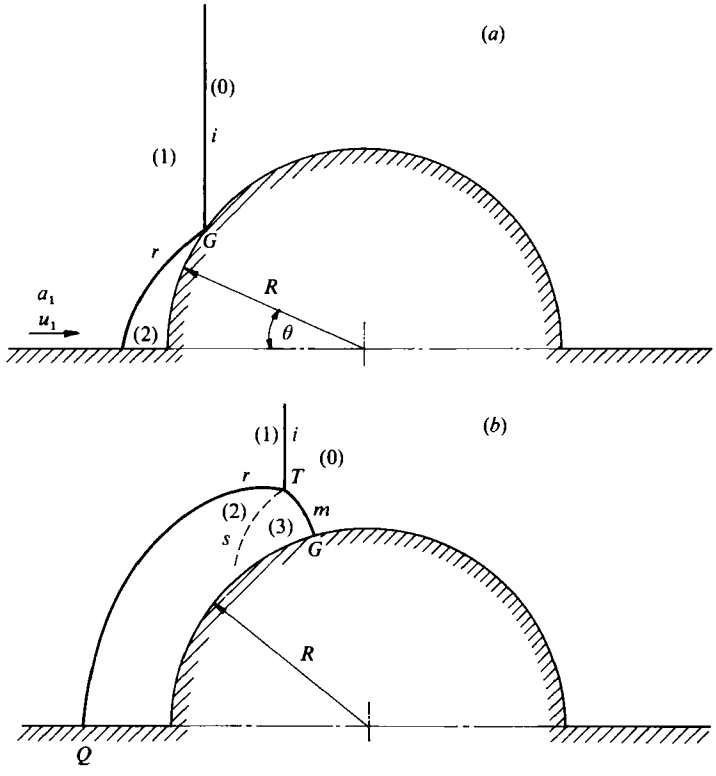

FIGURE 10. Schematic illustration of (*a*) a regular reflection over a cylindrical convex wedge, and (*b*) a Mach reflection over a cylindrical convex wedge.

7. Cylindrical convex wedge

When a planar shock wave collides with a cylindrical convex wedge it initially reflects as a regular reflection (figure 10*a*). As the incident shock wave propagates up the reflecting wedge, the regular reflection terminates and becomes a Mach reflection (figure 10*b*).

It is our belief that the race between the corner-generated signals and the incident shock wave is the dominant factor in this transition phenomenon too. Unfortunately, however, this case is much more difficult than that of a reflection over a cylindrical concave wedge. This is due to the fact that for this case the flow at point 2 (figure 10*a*) passes through the portion of the reflected shock wave which was reflected head-on from the wedge. Consequently, the changes in the flow properties across this portion of the reflected shock wave *cannot* be neglected. Thus the assumption that $u+a = u_1+a_1$ in region 2 (figure 10*a*) is not valid and should not be made. As a matter of fact $u+a \gg u_1+a_1$. Instead $u+a$ as a function of θ must be known if one is to carry out an integration of the form $\int (u+a)\,dt$. To the best of our knowledge such data is unavailable.

8. Conclusions

Two formulas for predicting the wedge angle for transition from Mach to regular reflection over cylindrical concave wedges have been developed. Both are based on Hornung *et al.*'s (1979) conclusion that a Mach reflection can exist only if the corner signals generated at the tip of the wedge can catch up with the incident shock wave.

When the predictions of the two models were compared with the available experimental results it was found that one of them is appropriate in the range $1 < M_s < 1.1$, while the other is in good agreement with the experimental results in the range $M_s > 1.1$. The predicted transition angles of these two formulas are in better agreement with the available experimental results than the one existing transition line of Itoh *et al.* (1981). While the model of Itoh *et al.* is based on Milton's (1975) modification of Whitham's (1957) theory, and hence is quite complicated to use, the present analysis results in two simple formulas which are very easy to apply.

An attempt was made to modify the developed transition formula to include the effect of the initial wedge angle. Although the modification shifted the transition line in the correct direction it failed to reproduce accurately enough the experimental results, probably due to the assumption, which for this situation is too crude, that the changes in the flow properties are negligible when it passes through the reflected shock wave.

Some limitation of the present model arising from the simplifying assumptions have been pointed out. In particular, the case of the reflection over a cylindrical convex wedge was considered. It is our belief that the present method should, in principle, be valid also for cylindrical convex wedges. However for that case the incident shock collides head-on with the wedge at its tip, resulting in a strong reflected shock wave across which the assumption given by (2) is invalid. Alternatively, the exact distribution of $u+a$ must be known.

As a final remark, it should be stressed that the present analytical transition formulas failed to account for the radius of curvature of the cylindrical wedge which is known to have an influence on the transition wedge angle.

The authors would like to thank Professor R. J. Sandeman from the Australian National University for his constructive remarks concerning the 'corner signal' concept. His comments were integrated into this paper. The authors wish to express their gratitude to Mr O. Onodera for carrying out the experiments. Finally, the encouragement of Professor M. Honda from the Institute of High Speed Mechanics, Tohoku University, Sendai, Japan, is highly appreciated.

REFERENCES

Ben-Dor, G. 1980 *AIAA J.* **18**, 1143.

Ben-Dor, G. & Glass, I. I. 1979 *J. Fluid Mech.* **92**, 459.

Ben-Dor, G. & Takayama, K. 1981 *Can. Aero. & Space J.* **27**, 128.

Ben-Dor, G., Takayama, K. & Kawauchi, T. 1980 *J. Fluid Mech.* **100**, 147.

Dewey, J. M., Walker, D. K., Lock, G. D. & Scotten, L. N. 1983 In *Shock Tubes and Waves* (ed. R. D. Archer & B. E. Milton), pp. 144–149. Sydney Shock Tube Symposium Publishers.

Heilig, W. H. 1969 *Phys. Fluids Suppl.* **12**, I, 154.

Henderson, L. F. & Lozzi, A. 1975 *J. Fluid Mech.* **68**, 139.

Hornung, H. G., Oertel, H. & Sandeman, R. J. 1979 *J. Fluid Mech.* **90**, 541.

ITOH, S. & ITAYA, M. 1979 In *Shock Tubes and Waves* (ed. A. Lifshitz & J. Rom), pp. 314–323. The Magnes Press, Hebrew University.

ITOH, S., OKAZAKI, N. & ITAYA, M. 1981 *J. Fluid Mech.* **108**, 383.

MILTON, B. E. 1975 *AIAA J.* **13**, 1531.

TAKAYAMA, K. & BEN-DOR, G. 1983 *Israel Journal of Technology* **21**, 197.

TAKAYAMA, K., BEN-DOR, G. & GOTOH, J. 1981 *AIAA J.* **12**, 1238.

TAKAYAMA, K. & SASAKI, M. 1983 *Rep. Inst. High Speed Mech., Tohoku Univ.*, Vol. 46. Sendai, Japan.

VON NEUMANN, J. 1963 *Collected Works*, Vol. 6. Pergamon.

WHITHAM, G. B. 1957 *J. Fluid Mech.* **4**, 337.